

Specific-heat measurements of superconducting NbS₂ single crystal in an external magnetic field: Study on the energy gap structure

J. Kačmarčík¹, Z. Pribulová¹, C. Marcenat^{1,2}, T. Klein^{3,4}, P. Rodière³, L. Cario⁵, and P. Samuely¹

¹*Centre of Very Low Temperature Physics at Institute of Experimental Physics, Slovak Academy of Sciences, Watsonova 47, SK-04001 Košice, Slovakia*

²*CEA-Institut Nanosciences et Cryogénie/ UJF-Grenoble 1, SPSMS, UMR-E 9001, LaTEQS, 17 rue des martyrs, 38054 GRENOBLE, France*

³*Institut Néel, CNRS, 38042 Grenoble, France* ⁴*Institut Universitaire de France and Université Joseph Fourier, 38041 Grenoble, France*

⁵*Institut des Matériaux Jean Rouxel, Université de Nantes-CNRS, 44322 Nantes, France*

(Dated: November 2, 2018)

The heat capacity of a 2H-NbS₂ single crystal has been measured by a highly sensitive ac technique down to 0.6 K and in magnetic fields up to 14 T. At very low temperatures data show excitations over an energy gap ($2\Delta_S/k_B T_c \approx 2.1$) much smaller than the BCS value. The overall temperature dependence of the electronic specific heat C_e can be explained either by the existence of a strongly anisotropic single-energy gap or within a two-gap scenario with the large gap about twice bigger than the small one. The field dependence of the Sommerfeld coefficient γ shows a strong curvature for both principal-field orientations, parallel ($H||c$) and perpendicular ($H \perp c$) to the c axis of the crystal, resulting in a magnetic field dependence of the superconducting anisotropy. These features are discussed in comparison to the case of MgB₂ and to the data obtained by scanning-tunneling spectroscopy. We conclude that the two-gap scenario better describes the gap structure of NbS₂ than the anisotropic s -wave model.

I. INTRODUCTION

The old concept of multiband/multigap superconductivity [1] has found its strong experimental evidence only recently in the rich physics of magnesium diboride [2]. Consequently more superconductors are (re)considered along this line. One of the important examples are the iron pnictides, a new class of high- T_c superconductors [3] for which multigap superconductivity is suggested to lead to an exotic pairing mechanism with a sign reversal of the order parameter between separated Fermi-surface sheets. A revision in dichalcogenides brings more and more signatures of a distribution of superconducting energy gaps, which can be either due to different gaps on different Fermi-surface sheets or anisotropic single gap.

Transition-metal dichalcogenides 2H-MX₂ (M = Nb, Ta, X = S, Se) are materials with layered structure. Nb or Ta atoms are trigonally prismatic coordinated by chalcogen atoms and metallic layers are held together by weak van der Waals forces. Because of this layered structure, electrical, magnetic, and optical properties show a high degree of anisotropy. NbS₂ is the only member of the 2H-MX₂ family, which does not undergo a charge-density wave transition [4]. This could be a reason for its strong anisotropy, much larger than that of NbSe₂.

NbSe₂ had been considered for a long time as being a conventional type II superconductor [5]. Later on, effects of the anisotropic and strong coupling interactions were taken into account [6, 7]. Recent measurements sensitive to the order parameter show evidence that more than one energy scale is necessary to account for establishing superconductivity [8–12]. NbS₂ was also originally

considered as just another anisotropic superconductor and its unusual specific heat dependence was not interpreted in detail [13, 14]. An important breakthrough came with scanning tunneling microscopy/spectroscopy (STM) measurements by Guillaumon et al. [15], showing strong indications for two superconducting energy gaps instead of a single anisotropic one. Since STM is a surface probe, this strong statement certainly needs independent support showing that the two gaps are reflecting the bulk properties of the system. In this paper we address this issue with bulk thermodynamic measurements of the specific heat at temperatures down to 0.6 K and in magnetic fields up to 14 Tesla via ac-calorimetry technique. We find that the electronic specific heat C_e cannot be described by the standard BCS model with a single isotropic energy gap. First, at the lowest temperatures the data shows that quasiparticles are excited over an energy gap much smaller than the BCS weak coupling limit. The overall temperature dependence of C_e can be described only if two gaps or an anisotropic one gap case is considered. Second, the field dependence of the Sommerfeld coefficient γ shows a strong curvature in striking similarity with that of NbSe₂ and MgB₂. However, the anisotropy of γ decreases with magnetic field in an opposite manner compared to the latter system. Finally, the two gap scenario is supported by the absence of in-plane gap anisotropy in recent STM imaging of the vortex lattice in NbS₂ [15], and by the fact that the numerical values of the two gaps obtained from fitting our data, $2\Delta_S/k_B T_c \approx 2.1$ and $2\Delta_L/k_B T_c \approx 4.6$, are also in a very good agreement with the STM data.

II. EXPERIMENT

Details of the synthesis of the single crystalline samples can be found elsewhere [16]. The crystals used for the specific heat measurements come from the same batch as those used in the previous STM studies [15]. Their chemical composition was checked using an energy dispersive X-ray spectroscopy (EDS). Single crystals were also confirmed to be of 2H polytype by X-ray diffraction measurements. In our experiment a thin crystal with a well defined hexagonal shape and dimensions $500 \times 500 \times 30 \mu\text{m}$ was chosen.

Specific heat measurements have been performed using an ac technique as described elsewhere [17]. The high sensitivity of this technique is not only very well adapted to measure the specific heat of very small samples but also to carry continuous measurements during temperature or magnetic field sweeps. We were thus able to obtain the field dependence of the electronic part of C/T at $T \approx 0.6 \text{ K}$ which only differs from its zero temperature limit, the Sommerfeld coefficient γ , by about 2%. Measurements were performed with the magnetic field aligned along the two main crystallographic orientations, i.e. parallel and perpendicular to the basal ab plane of the sample. The temperature oscillations of the sample were recorded by a thermocouple calibrated in magnetic field using measurements on ultrapure silicon. We performed measurements at temperatures down to 0.6 K and in magnetic fields up to 8 T in the ^3He and ^4He refrigerators in Košice. Supplementary measurements up to 14 Tesla and down to 2 K were performed in Grenoble.

III. RESULTS AND DISCUSSION

Figure 1 displays the temperature dependence of the specific heat of the sample (plus addenda) in selected magnetic fields up to 8 T for $H||ab$ and up to 3 T for $H||c$. The thermodynamic superconducting transition temperature at zero field was determined from the local entropy balance around the phase transition giving $T_c = 6.05 \text{ K}$. The zero-field anomaly at the transition is sharp ($\Delta T_c \sim 0.4 \text{ K}$) indicating the high quality and homogeneity of the sample. The position of the specific-heat jumps are gradually shifted toward lower temperatures for increasing magnetic field. Despite a significant broadening at high fields, the anomaly remains well resolved at all fields. A field of 3 Tesla applied along the c -axis was sufficient to completely suppress superconductivity in all the temperature range. On the other hand, 8 Tesla applied along the ab -planes shifts the superconducting anomaly down to only about 3-4K underlying the strong anisotropy of this system.

Later we extended the measurements down to 0.6 K in a ^3He fridge where the specific heat was measured at zero field and at $H||c = 3 \text{ T}$. In the case of a very small crystal like ours, it is difficult to evaluate the exact total contribution of the addenda. The electronic part of the

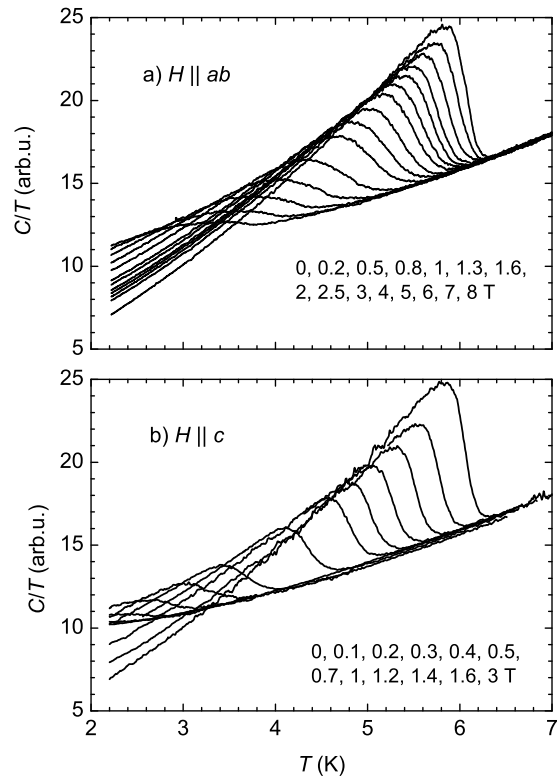


FIG. 1: a) Total specific heat C/T of NbS_2 in magnetic field parallel (a) and perpendicular (b) to the ab planes. In both data sets the zero field measurement is the rightmost curve.

total specific heat value can be obtained by extrapolation of C_{tot}/T for T approaching zero. This value corresponds to $\sim 38\%$ of γ_n , with $\gamma_n T$ being the electronic heat capacity of the sample in the normal state. To avoid any fitting procedures, the addenda and the phononic contributions have been eliminated by subtracting the data taken at $H||c = 3 \text{ T}$ from all the other runs. Thus, the electronic specific heat of the sample, $C_e(T)$, normalized to its normal state value, $\gamma_n T$, can be obtained experimentally by: $C_e(T)/\gamma_n T = \frac{\Delta(C/T)}{\gamma_n} + 1$, where $\Delta(C/T) = (C(T, H = 0)/T - C(T, H = 3\text{T}||c)/T)$ and $\gamma_n = C(H = 3\text{T}||c)/T|_{0.6\text{K}} - C(H = 0)/T|_{0.6\text{K}}$. The result is presented in Fig. 2 by the open circles. The only assumption in this procedure is the absence of magnetic field dependence of the addenda. This has been previously verified in numerous experiments using the same thermocouple wires and also confirmed here independently by the entropy conservation required for a second order phase transition, proving the thermodynamic consistency of the data and its treatment.

We first compare the electronic specific heat with the isotropic single gap (ISG) BCS model. The dashed line in Fig. 2 presents the ISG BCS specific heat (weak coupling of $2\Delta/k_B T_c = 3.52$). One can see that while the height of the jump at T_c of the experimental data is quite

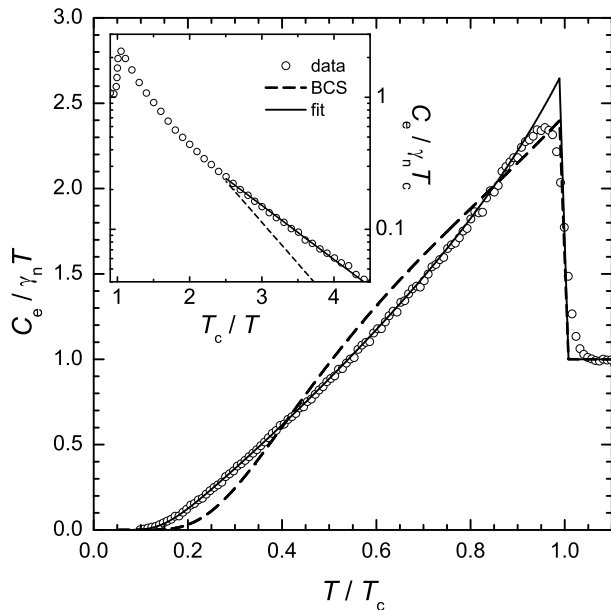


FIG. 2: Open circles: Electronic specific heat of NbS₂ in zero magnetic field extended down to 0.6 K. Dashed line: BCS single-gap weak-coupling case. Solid line: two-gap model with $2\Delta_S/k_B T_c = 2.1$, $2\Delta_L/k_B T_c = 4.6$ and respective relative contributions $\gamma_S/\gamma_n = 0.4$, $\gamma_L/\gamma_n = 0.6$. The anisotropic gap model with anisotropy parameter $\alpha = 0.5$ and $2\Delta_0/k_B T_c = 3.6$ follows essentially the same line. Inset: exponential dependence of the specific heat, the full line represents the best fit of the exponential decay, the dashed line is the behavior expected for a BCS single-gap weak-coupling limit.

well reproduced, a significant deviation occurs at lower temperatures. The discrepancy between the BCS curve and the measured data represents 18 % (7 %) of the total signal at 1.4K (4K), which is significantly larger than the error bars of our measurements.

The inset of Fig. 2 displays the logarithm of the electronic specific heat versus T_c/T . As shown, one obtains an exponential dependence $C_e \propto \exp(-b * T_c/T)$ for $T_c/T \geq 2.5$. However, the parameter b is significantly lower than the value expected for the BCS weak coupling limit in the temperature range $T_c/T = 2.5 - 4.5$ [18]. This corresponds to coupling ratio $2\Delta/k_B T_c \sim 2.3$ that is much smaller than the ISG BCS value of 3.52, indicating that the quasiparticles are activated over a small energy gap. This fact as well as the overall shape of the specific heat temperature dependence resembles the case of MgB₂.

A phenomenological α -model of the specific heat accounting for independent contributions from two bands with two different energy gaps has been successfully applied in the case of MgB₂ [19]. The magnitude of the small gap $2\Delta_S/k_B T_c$ and of the large gap $2\Delta_L/k_B T_c$ at $T = 0$ are fitting parameters of the model. The third parameter is the relative fraction of the density of states of the two bands $\gamma_{S,n}/\gamma_{L,n}$. The full line in Fig. 2 repre-

sents a fit to the experimental data yielding the following parameters: $2\Delta_S/k_B T_c = 2.1 \pm 0.05$, $2\Delta_L/k_B T_c = 4.6 \pm 0.2$, and $\gamma_{S,n}/\gamma_{L,n} = 0.67 \pm 0.15$. The value of the small gap is close to the one evaluated from the exponential decay shown in the inset of Fig. 2. Importantly, both gap values are in striking agreement with those found in the STM experiment [15] confirming that the latter are characteristic of the bulk.

As previously shown by Huang et al. [10], the temperature dependence of the specific heat of NbSe₂, another two-gap superconductor, can also be described by an anisotropic s -wave model, where the gap anisotropy is supposed to be in the form of $\Delta = \Delta_0(1 + \alpha \cos 6\phi)$ corresponding to the hexagonal in-plane symmetry. Here, Δ_0 is the average gap value and α denotes its anisotropy, yielding $\Delta_{max} = \Delta_0(1 + \alpha)$ and $\Delta_{min} = \Delta_0(1 - \alpha)$. This model with parameters $\alpha = 0.5$ and $2\Delta_0/k_B T_c = 3.6$ fits our data as well as the two gap scenario, *the difference between the two models is negligible*. We remark that the anisotropic gap should leave its footprint in the anisotropic vortex core ξ as it is proportional to the related Fermi velocity v_F divided by the gap at zero temperature $\Delta(0)$. However, in contrast to NbSe₂, for which STS images revealed a sixfold star shape of the vortex cores, the fully isotropic vortices have been imaged in NbS₂ [15] questioning the applicability of the anisotropic single gap model in our case.

We have measured thoroughly the evolution of the specific heat in the mixed state. At $T = 0.6$ K the electronic specific heat term C_e/T is very close to the Sommerfeld coefficient γ . Its field dependence is displayed in Fig. 3a and 3b for both principal field orientations. Our maximum field available at this temperature range (8 Tesla) was not sufficient to reach the normal state for $H||ab$, but it was well above the upper critical field value of 2.4 ± 0.1 Tesla for $H||c$. Fig. 3a emphasizes the strong non-linearity of $\gamma(H)$ when H is applied perpendicular to the ab plane. Again, such a non-linearity could be associated with the existence of 2 gaps or a single anisotropic one.

The increase of γ with magnetic field is mainly due to the quasiparticle contribution inside the vortex cores. In the case of superconductor with a single isotropic gap, γ should increase linearly in small magnetic field and a small nonlinearity in $\gamma(H)$ appears above the field where flux lines start overlapping. According to the calculations of Nakai et al. [20], much stronger non-linearity of $\gamma(H)$ is achieved in case of anisotropic-gap superconductors. The full line in the Fig. 3a displays the field dependence of the normalized density of states $N(B)/N_0$ (proportional to the Sommerfeld coefficient) calculated by Nakai et al. for the anisotropic gap with $\alpha = 0.5$. The model qualitatively reproduces the behavior in our data (open circles), but fails to describe the fast increase of $\gamma(H)$ at low fields. This is evident in the inset of Fig. 3a where the derivative $\partial N(B)/\partial B$, i.e. the slope of $N(B)$ for $\alpha = 0.5$ (line) and the slope of measured Sommerfeld coefficient $\partial \gamma(H)/\partial H$ (open circles) are compared. This

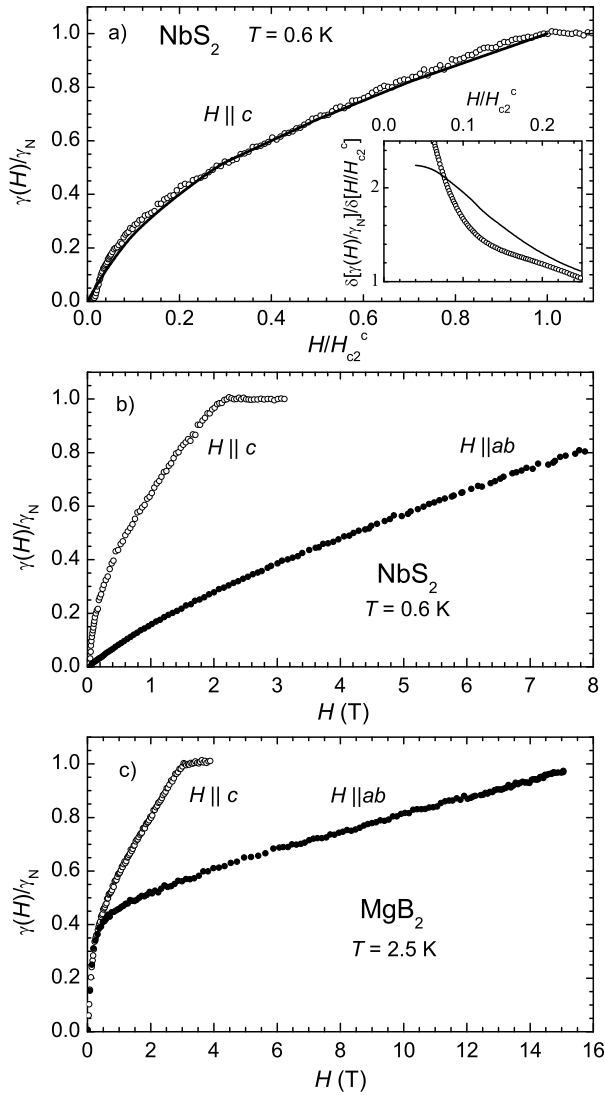


FIG. 3: (a) Open circles - normalized Sommerfeld coefficient γ as a function of magnetic field perpendicular to the ab planes of NbS₂. Line - model accounting for highly anisotropic gap with $\alpha = 0.5$ [20]. Inset is the derivative of the corresponding curves from the main panel: open circles - of the measured data, line - of the model. (b) and (c) γ/γ_N for both orientations of the magnetic field in NbS₂ and MgB₂ [21], respectively.

discrepancy makes the explanation of the specific heat data by the anisotropic gap scenario rather inconsistent. The observed $\gamma(H)$ behavior resembles the two-gap case of MgB₂ (see Fig. 3c, left curve) [21], where the initial rapid increase of $\gamma(H)$ due to dominant role of the π band with the small gap changes at fields where the σ band with the large gap comes into play.

Next, we compare the behavior of the Sommerfeld coefficients in magnetic fields applied parallel and perpendicular to the basal planes of the both materials, NbS₂ (Fig. 3b) and MgB₂ (Fig. 3c). The latter is taken from

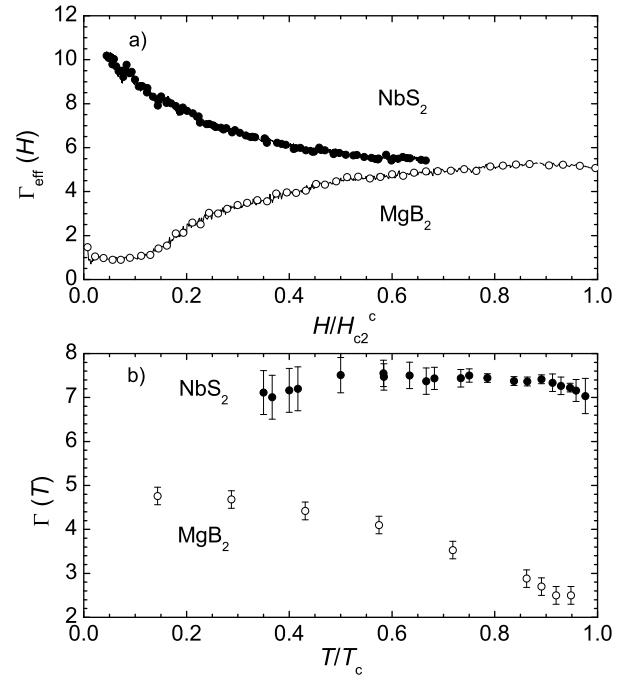


FIG. 4: Anisotropy of NbS₂ (full circles) compared to MgB₂ [21, 27] (open circles): (a) field dependence of effective anisotropy defined as the ratio of the fields applied in both principal orientations that correspond to the same γ value in Fig.3b and Fig. 3c (b) temperature dependence of anisotropy $\Gamma = H_{c2}^{ab}/H_{c2}^c$.

Ref.[21]. Following the procedure introduced by Bouquet et al. in Ref.[22] an effective anisotropy Γ_{eff} can be obtained from these $\gamma(H)$ dependences. It is defined as the ratio of the magnetic fields in the ab plane and along the c axis yielding the same γ value in Fig. 3b and Fig. 3c. Γ_{eff} is plotted in Fig 4a for both compounds as a function of the field $H \parallel c$ normalized to its upper critical field value $H_{c2} \parallel c$. As discussed already in the work of Bouquet et al. on MgB₂ [22] the choice of the abscissa is arbitrary. We chose $H \parallel c$, but we could plot Γ_{eff} versus $H \parallel ab$ or versus $\gamma(H)$ as well. Note that this Γ_{eff} tends towards the usual anisotropy of H_{c2} , $\Gamma = \frac{H_{c2}^{ab}}{H_{c2}^c}$ when $\frac{\gamma}{\gamma_n} \rightarrow 1$ at large magnetic fields. In MgB₂ at low fields ($\frac{H}{H_{c2}^c} < 0.1$), the $\gamma(H)$ curves for the two principal directions are practically identical which gives $\Gamma_{eff} = 1$ as shown in Fig. 4a. At larger fields, Γ_{eff} increases reflecting a reduced contribution from the isotropic π -band, reaching $\Gamma_{eff} \sim 5$ which is the anisotropy of the dominant σ -band [21]. In NbS₂, one observes an opposite field dependence of Γ_{eff} which starts from a highly anisotropic value $\Gamma_{eff} \sim 10$ at low fields and decreases to $\Gamma_{eff} \sim 5.5$ at our maximum field. A field dependent superconducting anisotropy is a typical signature of multigap superconductivity where a role of bands with different gaps can significantly vary with magnetic field [23–25]. In contrast to MgB₂ case, in

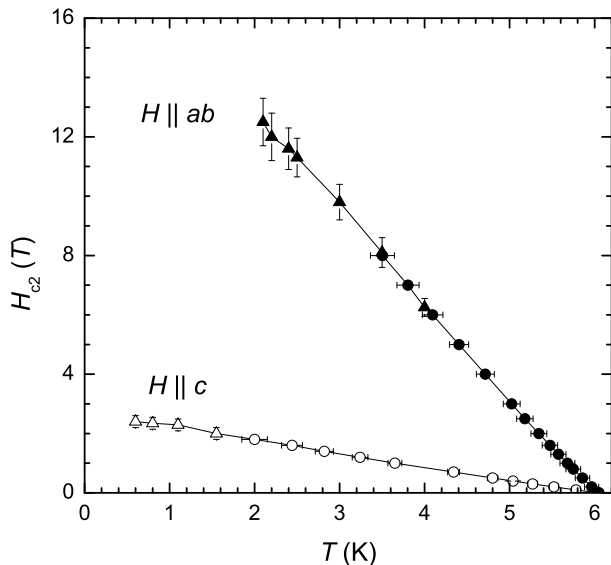


FIG. 5: Upper critical field H_{c2} for magnetic field $\parallel ab$ (full circles result from temperature-sweep measurements, full triangles from field sweeps) and $\parallel c$ (open circles result from temperature-sweep measurements, open triangles from field sweeps).

NbS_2 both bands would be anisotropic, as suggested by analogy with NbSe_2 in which band structure calculations [26] show mostly 4 Fermi surface sheets derived from Nb d -bands forming warped cylinders along the c axis, centered on the Γ and K points in the Brillouin zone. Moreover, two sheets derived from the bonding Nb d band are significantly more warped than the two derived from the antibonding Nb d band. Different warping of Nb sheets can naturally lead to a different level of anisotropy in each band. Thus, a qualitatively different behavior of $\Gamma_{eff}(H)$ compared to MgB_2 can be expected.

Finally, we inspected the upper critical magnetic fields for both principal orientations of magnetic field. Fig. 5 summarizes the values of H_{c2} derived from the temperature-sweep measurements of the specific heat shown in Fig. 1, as well as from field-sweep measurements. Two sets of field-sweeps were performed, one in 14 Tesla magnet for $H \parallel ab$ in a temperature range down to 2 K, and another one taken in the ^3He cryostat down to 0.6 K in the 8 Tesla coil. As stated above, we determined T_c at zero field from the local entropy balance around the anomaly. However, at finite fields this definition is not very practical for establishing $T_{c2}(H)$, or $H_{c2}(T)$. In order to reduce the uncertainty of the H_{c2} value arising from the broadening of the transition particularly at lower temperatures (higher fields), we inspected the temperature shift between two neighboring curves in Fig. 1. A similar procedure was used to determine H_{c2} from field-sweep measurements. The resulting temperature dependence of H_{c2} is shown in Fig. 5 for both $H \parallel ab$ and $H \parallel c$.

Importantly, the three independent sets of temperature and field-sweeps measurements yield consistent results with a nice overlap. Both temperature dependencies show a slight positive curvature for temperatures $T > T_c/2$. The upper critical field in the ab plane reveals very high values with dH_{c2}/dT slope of about 3 Tesla/K, close to the Pauli paramagnetic limit.

The temperature dependence of the superconducting anisotropy Γ calculated as a ratio $H_{c2} \parallel ab / H_{c2} \parallel c$ of the upper critical fields is displayed in Fig. 4b together with the results obtained in MgB_2 [27]. As shown, in contrast to MgB_2 , the resulting anisotropy Γ is close to 7 and approximately constant for $T/T_c > 0.3$. Note that this value might be slightly underestimated in case of a small misalignment of the crystal for $H \parallel ab$. Our results are consistent with those obtained by Onabe et al. [28] from resistive measurements in a field up to 2 Tesla. The strong decrease of Γ in MgB_2 close to T_c is a direct consequence of the existence of the isotropic π -band. This is not a general feature of multiband superconductivity since $\Gamma(T)$ results from a subtle balance between the Fermi velocities and the relative weight in the DOS of the different bands [24]. These precise calculations are still to be carried out in the case of NbS_2 .

IV. CONCLUSIONS

Analysis of the zero-field specific heat data has shown that: (1) the zero-field electronic term of the specific heat cannot be described by an isotropic single-gap BCS formula, but it is compatible with the two-gap α model; (2) the large (small) gap is $2\Delta_L/k_B T_c \approx 4.6$ ($2\Delta_S/k_B T_c \approx 2.1$). The measurements in the mixed state have supported the two-gap scenario revealing: (3) a strongly non-linear $\gamma(H)$; (4) a field-dependent superconducting anisotropy. Even if some of these features of the specific heat could be eventually explained by an extremely anisotropic-gap superconducting model, this would not be compatible with the observation of two well-resolved gap features with sizes of $2\Delta_S/k_B T_c \approx 2$ and 4, respectively, and also with the absence of in-plane anisotropy in the vortex lattice images by the scanning-tunneling spectroscopy of Guillaumón et al. To conclude, our bulk thermodynamic measurements are in full agreement with STM spectra, supporting that NbS_2 is another case of well resolved two-gap superconductor.

Acknowledgments

This work was supported by the EC Framework Programme MTKD-CT-2005-030002, by the EU ERDF (European regional development fund) grant No. ITMS26220120005, by the Slovak Research and Development Agency, under Grants No. VVCE-0058-07, No. APVV-0346-07, No. SK-FR-0024-09 and No. LPP-0101-06, and by the U.S. Steel Košice, s.r.o. Centre of Low

Temperature Physics is operated as the Centre of Excellence of the Slovak Academy of Sciences. We thank G.

Karapetrov for careful reading of the manuscript.

-
- [1] H. Suhl, B. T. Matthias, and L. R. Walker, *Phys. Rev. Lett.* **3**, 552 (1959).
- [2] X. X. Xi, *Rep. Prog. Phys.* **71**, 116501 (2008).
- [3] *Superconductivity in Iron-Pnictides*, eds. P. C. W. Chu et al., *Physica C* **469**, 313-674 (2009).
- [4] D. E. Moncton, J. D. Axe, and F. J. DiSalvo, *Phys. Rev. Lett.* **34**, 734 (1975).
- [5] B. T. Matthias, T. H. Geballe, and V. B. Compton, *Rev. Mod. Phys.* **35**, 1 (1963).
- [6] N. Kobayashi, K. Noto, and Y. Muto, *J. Low. Temp. Phys.* **27**, 217 (1977).
- [7] D. Sanchez, A. Junod, J. Muller, H. Berger and F. Lèvy, *Physica B* **204**, 167 (1995).
- [8] T. Yokoya, T. Kiss, A. Chainani, S. Shin, M. Nohara, and H. Takagi, *Science* **294**, 2518 (2001).
- [9] J. D. Fletcher, A. Carrington, P. Diener, P. Rodière, J. P. Brison, R. Prozorov, T. Olheiser, and R. W. Giannetta, *Phys. Rev. Lett.* **98**, 057003 (2007).
- [10] C. L. Huang, J.-Y. Lin, Y. T. Chang, C. P. Sun, H. Y. Shen, C. C. Chou, H. Berger, T. K. Lee, and H. D. Yang, *Phys. Rev. B* **76**, 212504 (2007).
- [11] T. Kiss, T. Yokoya, A. Chainani, S. Shin, T. Hanaguri, M. Nohara and H. Takagi, *Nature Physics* **3**, 720 (2007).
- [12] T. Valla, A.V. Fedorov, P. D. Johnson, P-A. Glans, C. McGuinness, K. E. Smith, E.Y. Andrei, and H. Berger, *Phys. Rev. Lett.* **92**, 086401 (1994).
- [13] Y. Hamaue and R. Aoki, *J. Phys. Soc. Jap.* **55**, 1327 (1986).
- [14] D.C. Dahn, J.F. Carolan, and R.R. Haering, *Phys. Rev. B* **33**, 5214 (1986).
- [15] I. Guillamón, H. Suderow, S. Vieira, L. Cario, P. Diener, and P. Rodière, *Phys. Rev. Lett.* **101**, 166407 (2008).
- [16] W. Fisher and M. Sienko, *Inorg. Chem.* **19**, 39 (1980).
- [17] P. F. Sullivan and G. Seidel, *Phys. Rev.* **173**, 679 (1968).
- [18] *Superconductivity*, edited by R. D. Parks, Marcel Dekker Inc., New York 1969.
- [19] F. Bouquet, Y. Wang, R. A. Fisher, D. G. Hinks, J. D. Jorgensen, A. Junod, and N. E. Phillips, *Europhys. Lett.* **56**, 856 (2001).
- [20] N. Nakai, P. Miranović, M. Ichioka, and K. Machida, *Phys. Rev. B* **70**, 100503(R) (2004).
- [21] Z. Pribulová, T. Klein, J. Marcus, C. Marcenat, F. Levy, M. S. Park, H. G. Lee, B. W. Kang, S. I. Lee, S. Tajima, and S. Lee, *Phys. Rev. Lett.* **98**, 137001 (2007).
- [22] F. Bouquet, Y. Wang, I. Sheikin, T. Plackowski, A. Junod, S. Lee, S. Tajima, *Phys. Rev. Lett.* **89**, 257001 (2002).
- [23] V. G. Kogan and S. I. Bud'ko, *Physica C* **385**, 131 (2003).
- [24] T. Dahm and N. Schopohl, *Phys. Rev. Lett.* **91**, 017001 (2003).
- [25] A. A. Golubov, A. Brinkman, O. V. Dolgov, J. Kortus, and O. Jepsen, *Phys. Rev. B* **66**, 054524 (2002).
- [26] M. D. Johannes, I. I. Mazin, and C. A. Howells, *Phys. Rev. B* **73**, 205102(2006).
- [27] L. Lyard, P. Samuely, P. Szabo, T. Klein, C. Marcenat, L. Paulius, K. H. P. Kim, C. U. Jung, H.-S. Lee, B. Kang, S. Choi, S.-I. Lee, J. Marcus, S. Blanchard, A. G. M. Jansen, U. Welp, G. Karapetrov, and W. K. Kwok, *Phys. Rev. B* **66**, 180502(R) (2002).
- [28] K. Onabe, M. Naito, and S. Tanaka, *Journal of the Phys. Soc. of Japan* **45**, 50 (1978).